

Electronic Supplementary Information for

One-pot selective conversion of C5-furan into 1,4-pentanediol over bulk Ni-Sn alloy catalysts in an ethanol/H₂O solvent mixture†

Rodiansono,^{*a} Maria Dewi Astuti,^a Takayoshi Hara,^b Nobuyuki Ichikuni,^b and Shogo Shimazu^{*b}

^aDepartment of Chemistry, Lambung Mangkurat University, Jl. A. Yani Km 36 Banjarbaru, Indonesia 70714. Tel./fax: +62 511 477 3112.

^bGraduate School of Engineering, Chiba University, 1-33 Yayoi, Inage, Chiba 263-8522, Japan, Tel./fax: +81 43 290 3379.

Corresponding authors: rodiansono@ulm.ac.id (R. Rodiansono). Tel./fax: +62 511 477 3112 and shimazu@faculty.chiba-u.jp (S. Shimazu)

Contents

1. Experimental sections (catalyst preparation, characterization, and procedure of catalytic activity test)
2. Bulk compositions, BET surface area (S_{BET}), Ni active surface area (S_{Ni}), and Ni-Sn alloy crystallite size (**Table S1**)
3. XRD patterns of Ni-Sn alloys with different Ni/Sn ratio (**Fig. S1**)
4. Ni K-edge XANES spectra for (a) Ni₄Sn, (b) Ni₃Sn (c) Ni₃Sn₂, (d) Ni₃Sn₄ (**Fig. S2**)
5. Le Bail intensity extraction profiles of Powder XRD data for Ni-Sn(3.0) alloy catalyst (**Fig. S3**)
6. Le Bail intensity extraction profiles of powder XRD data for Ni-Sn(1.5) alloy catalyst (**Fig. S4**)
7. Le Bail intensity extraction profiles of powder XRD data for Ni-Sn(0.75) alloy catalyst (**Fig. S5**)
8. NH₃-TPD spectra of bulk Ni-Sn alloy catalysts (**Fig. S6**)
9. Results of catalytic reactions of various substrates over Ni-Sn(1.5) alloy catalysts (**Table S2**)
10. Comparison of the present work with reported-literatures for the synthesis of 1,4-PeD from C5-furan compounds (**Table S3**)
11. The proposed reaction mechanism for 1,4-PeD synthesis from C5-furan over bulk Ni-Sn alloy catalysts (**Scheme S1**)
12. Hydrogenation of 5H₂PeO to 1,4-PeD over bulk Ni-Sn alloy catalysts (**Scheme S2**)
13. ¹H NMR of the crude yield of 1,4-pentanediol (after removal of solvent) (**Fig. S7**)
14. ¹H NMR of the isolated yield of 1,4-pentanediol (**Fig. S8**)
15. ¹³C-NMR of the isolated yield of 1,4-pentanediol (**Fig. S9**)
16. ¹H NMR of the synthesised 1,4-pentanediol from 5-hydroxy-2-pentanone (**Fig. S10**)
17. ¹³C NMR the synthesised 1,4-pentanediol from 5-hydroxy-2-pentanone (**Fig. S11**)
18. XRD patterns of the recovered Ni-Sn(1.5) alloy catalyst before and after reactivated by H₂ treatment at 673 K for 1.5 h (**Fig. S12**)
19. References

1. Experimental sections

Materials

NiCl₂·6H₂O (98%) and SnCl₂·2H₂O (99.9%), ethanol (99.5%), and 2-methoxyethanol (99.8%) were purchased from WAKO Pure Chemical Co. and used as received. Furfuraldehyde (98%), furfuryl alcohol (97%), 2-methyl furan (98%) and tetrahydro furfuryl alcohol (99%) were purchased from Tokyo Chemical Industry Co. All organic chemical compounds were purified using standard procedures prior to use.¹

Details of procedures in the synthesis of bulk Ni-Sn(1.5) alloy^{S1}

Bulk Ni-Sn(1.5) alloy was synthesized from the mixture of nickel (II) chloride hexahydrate and tin (II) chloride dihydrate solution. NiCl₂·6H₂O was dissolved in deionized water (denoted as solution A) and SnCl₂·2H₂O was dissolved in ethanol/2-methoxy ethanol (2:1) (denoted as solution B) at room temperature under gentle stirring. Solution A and B were mixed at the room temperature, then the temperature was raised to 323 K and kept in stirring for 12 h. The pH was adjusted to 11~12 by addition dropwise of an aqueous solution NaOH. The mixture was transferred to the sealed-Teflon autoclave reactor for hydrothermal processes at 423 K for 24 h. The obtaining black solid precipitate was washed with distilled water and acetone and then dried *in vacuo* for overnight. Prior to characterization and catalytic reaction, the black solid of Ni-Sn alloy was treated by hydrogen at 673 K for 1-1.5 h.

Details of procedures in the synthesis of R-Ni/AlOH^{S2}

The typical procedure of the synthesis of Raney nickel supported on aluminum hydroxide catalyst (denoted as R-Ni/AlOH) is described as follows: Raney Ni-Al alloy powder (1.0 g) was slowly added to a dilute aqueous solution of NaOH (0.31 M, 8 mL) at room temperature. The temperature was raised to 363 K and 1 mL of 3.1 M NaOH solution was subsequently added and stirred for 30 min. The mixture was placed into a sealed-Teflon autoclave reactor for hydrothermal treatment at 423 K for 2 h. The resulting precipitate was filtered, washed with distilled water until the filtrate was neutralized, and then stored in water. The catalyst was dried under vacuum before the catalytic reaction.

Details of procedure in the catalytic reaction of furfuraldehyde (FFald), furfuryl alcohol (FFalc), and 2-methyl furan (2-MTF)

A typical reaction of furfuraldehyde was carried out in the following manner. Furfural (1.2 mmol) in ethanol/H₂O 1.5/2.0 v/v (3.5 mL) solvent mixture, decalin (0.25 mmol) as an internal standard, were placed into an autoclave reactor system of Taiatsu Techno (a Pyrex tube was fitted inside of a sus316 jacket to protect the vessel from corrosion in acidic media). After H₂ was introduced into the reactor (initial pressure of H₂ was 3.0 MPa) at room temperature, the temperature of the reactor was raised to 453 K for 12 h. In the reaction, 1,4-pentanediol (1,4-PeD), furfuryl alcohol (FFalc), tetrahydro furfuryl alcohol (THFalc), and 2-hydroxy-2-methyl tetrahydro furan (2H2MTHF) were mainly produced and 2-methyl tetrahydro furan (2-MTHF), 1,2-pentanediol (1,2-PeD), 1,5-pentanediol (1,5-PeD) were also detected.

In the case of the catalytic reaction of furfuryl alcohol, 1.1 mmol of furfuryl alcohol was dissolved in 3.5 mL ethanol/H₂O mixture and placed into an autoclave reactor system of Taiatsu Techno (a Pyrex tube was fitted inside of a sus316 jacket to protect the vessel from corrosion in acidic media). After H₂ was introduced into the reactor (initial pressure of H₂ was 3.0 MPa) at room temperature, the temperature of the reactor was raised to 433 K for 12 h. Experimental apparatus and reaction procedures are the same as the case of furfural. In the reaction, 1,4-PeD, 1,5-PeD, and 2H2MTHF were mainly produced. 1-PeOH and 2-PeOH were not detected over all the reaction.

In the case of the catalytic reaction of 2-methyl furan, 1.5 mmol of 2-methyl furan was dissolved in 3.5 mL ethanol/H₂O mixture and placed into an autoclave reactor system of Taiatsu Techno (a Pyrex tube was fitted inside of a sus316 jacket to protect the vessel from corrosion in acidic media). After H₂ was introduced into the reactor (initial pressure of H₂ was 3.0 MPa) at room temperature, the temperature of the reactor was raised to 433 K for 12 h. Experimental apparatus and reaction procedures are the same as the case of

furfural. In the reaction, 1,4-PeD, 2-MTHF were mainly produced, while 2H2MTHF and 2-PeOH and were also detected.

Analytical GLC was performed by a Shimadzu GC-8A with a flame ionization detector equipped with Silicone OV-101 packing (3 m). GC-MS was performed by a Shimadzu GC-17B with a thermal conductivity detector equipped with an RT- β DEXsm capillary column. ^1H NMR and ^{13}C NMR spectra were obtained on JNM-AL400 at 400 MHz in chloroform- d_1 or D_2O with TMS as an internal standard. Products were confirmed by the comparison of their GC and GC-MS retention time, mass, ^1H NMR and ^{13}C NMR spectra with the literatures, except for 2H2MTHF due to the limitation of commercial availability.

Details of procedure in the characterization of catalysts

Details of the ICP-AES analysis

The bulk compositions of the catalysts were determined by inductively coupled plasma-atomic emission spectroscopy (ICP-AES), using an SPS1700 HVR of SII instrument and the results are summarized in **Table S1**. The amount of metal leaching was measured from the solution after the reaction. We found that the Sn leaching ratio to the total Sn on the catalyst was determined to about 5%. On the other hand, the Ni leaching amount was below the detection limit of the ICP analysis, and the leaching ratio to the total Ni on the catalyst is <0.1% and the leaching of Ni was negligible.

Details of X-ray diffraction patterns

Powder X-ray diffraction was taken on a Mac Science M18XHF instrument using monochromatic $\text{CuK}\alpha$ radiation ($\lambda = 0.15418 \text{ nm}$). It was operated at 40 kV and 200 mA with a step width of 0.02° and a scan speed of 4° min^{-1} . The formation of Ni-Sn alloy for every sample was confirmed by JCPDS card.⁵³ The mean crystallite size of Ni-Sn was calculated from the full width at half maximum (FWHM) of the Ni-Sn alloy diffraction peak according to the Scherrer equation. $\text{Ni}_3\text{Sn}_2(110)$ for Ni-Sn(1.5) alloy, $\text{Ni}_3\text{Sn}(201)$ for Ni-Sn(3.0) alloy, and $\text{Ni}_3\text{Sn}_4(112)$ for Ni-Sn(0.75) alloy systems.

Ni K-edge X-ray absorption near edge structure (XANES)⁵⁴

X-ray absorption spectra around the Ni K-edges were recorded at the BL01B1 beamline of the SPring-8 (8 GeV, 100 mA) of the Japan Synchrotron Radiation Research Institute (Proposal No. 2010B 1100 by Professor Dr. Kiyotomi Kaneda, Graduate School of Engineering Science, Osaka University). A Si (311) two-crystal monochromator was used. Ion chambers filled with Ar(100%) and Ar(50%) /Kr(50%) were used for the I_0 and me detectors, respectively, and the samples were located between these ion chambers. Energy calibration was carried out using a Ni foil (30 mm of thickness). Ni K-edge XANES spectra of all samples were recorded in the step scan mode. Data reduction using the RE X2000 Ver.2.3.3 program (Rigaku) was carried out.

Details of the H_2 adsorption measurement

The active surface areas were determined by H_2 chemisorption. After the catalyst was heated at 393 K under vacuum for 30 min, it was heated at 673 K under H_2 for 30 min and under vacuum for 30 min, followed by evacuation to room temperature for 30 min. The adsorption of H_2 was conducted at 273 K. The active surface area was calculated from the volume of H_2 desorbed by assuming an H/Ni stoichiometry of one, respectively and a surface area of $6.77 \times 10^{-20} \text{ m}^2$ per atom Ni based on an equal distribution of the three lowest index planes of Ni-Sn.⁵⁵

2. Results of catalyst characterizations

Table S1 Bulk compositions, BET surface area (S_{BET}), Ni active surface area (S_{Ni}), alloy component, and Ni-Sn alloy crystallite size

Entry	Catalyst ^a	Bulk composition ^b	Alloy component ^c		$S_{\text{BET}}^{\text{d}}/\text{m}^2 \text{ g}^{-1}$	$S_{\text{Ni}}^{\text{e}}/(\text{m}^2 \text{ g}^{-1} \text{ g}^{-1}_{\text{cat}})$	Ni-Sn crystallite sizes ^f /nm
			Major	Minor			
1	Ni-Sn(4.0)	Ni _{79.9} Sn _{20.1}	Ni ₃ Sn	Ni ₃ Sn ₂	5.21	n.d	n.d
2	Ni-Sn(3.0)	Ni _{74.9} Sn _{25.1}	Ni ₃ Sn	Ni ₃ Sn ₂	5.10	2.9	13.4 ^g
3	Ni-Sn(2.0)	Ni _{66.2} Sn _{33.8}	Ni ₃ Sn ₂	NiSn, Ni ₃ Sn	4.50	n.d	n.d
4	Ni-Sn(1.5)	Ni _{59.9} Sn _{40.1}	Ni ₃ Sn ₂	NiSn, Ni ₃ Sn	12.02	2.0	17.3 ^h
5	Ni-Sn(1.0)	Ni _{50.0} Sn _{50.0}	Ni ₃ Sn ₂	NiSn, Ni ₃ Sn	n.d	n.d	n.d
6	Ni-Sn(0.75)	Ni _{42.7} Sn _{57.3}	Ni ₃ Sn ₄	NiSn	56.51	0.3	23.4 ⁱ

^a Values in the parenthesis indicate Ni/Sn molar ratio as the precursor amount. n.d. = not determined.

^b Determined by ICP-AES.

^c Compared to JCPDS-ICDD cards of the existing Ni-Sn alloy.⁵³

^d Determined by N₂ physisorption at 77 K.

^e Calculated from the volume H₂ desorbed by assuming H/Ni is 1 in stoichiometry.

^f The average crystallite sizes of Ni-Sn were calculated from the full width at half maximum (FWHM) of the Ni-Sn diffraction peak according to the Scherrer's equation.

^g Ni₃Sn(201)

^h Ni₃Sn₂(110)

ⁱ Ni₃Sn₄(112)

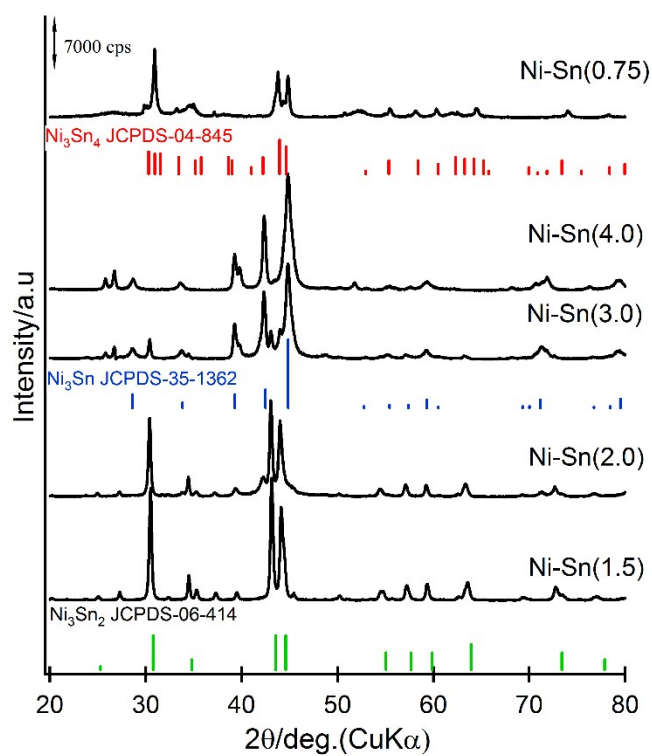


Fig. S1 XRD patterns of bulk Ni-Sn(1.5), Ni-Sn(2.0), Ni-Sn(3.0), Ni-Sn(4.0), and Ni-Sn(0.75) alloy catalysts compared with the prescribed JCPDS of authentic data.

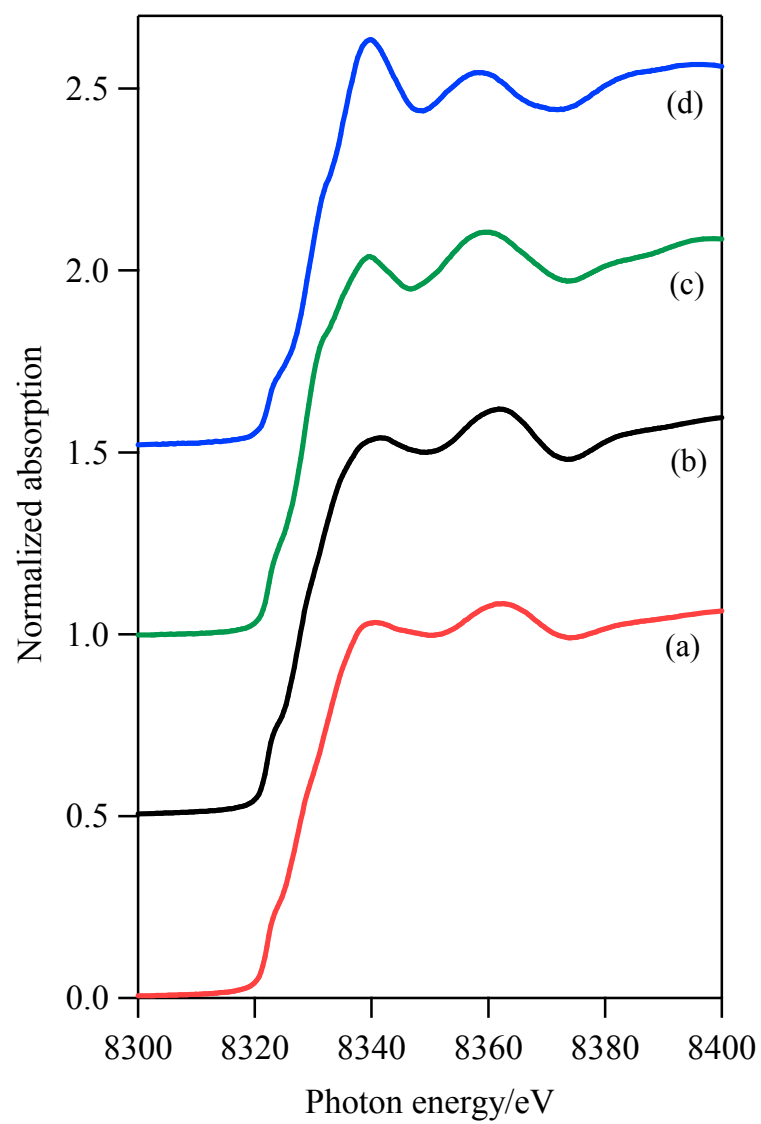


Fig. S2. Ni K-edge XANES spectra for (a) Ni_4Sn , (b) Ni_3Sn (c) Ni_3Sn_2 , (d) Ni_3Sn_4 .

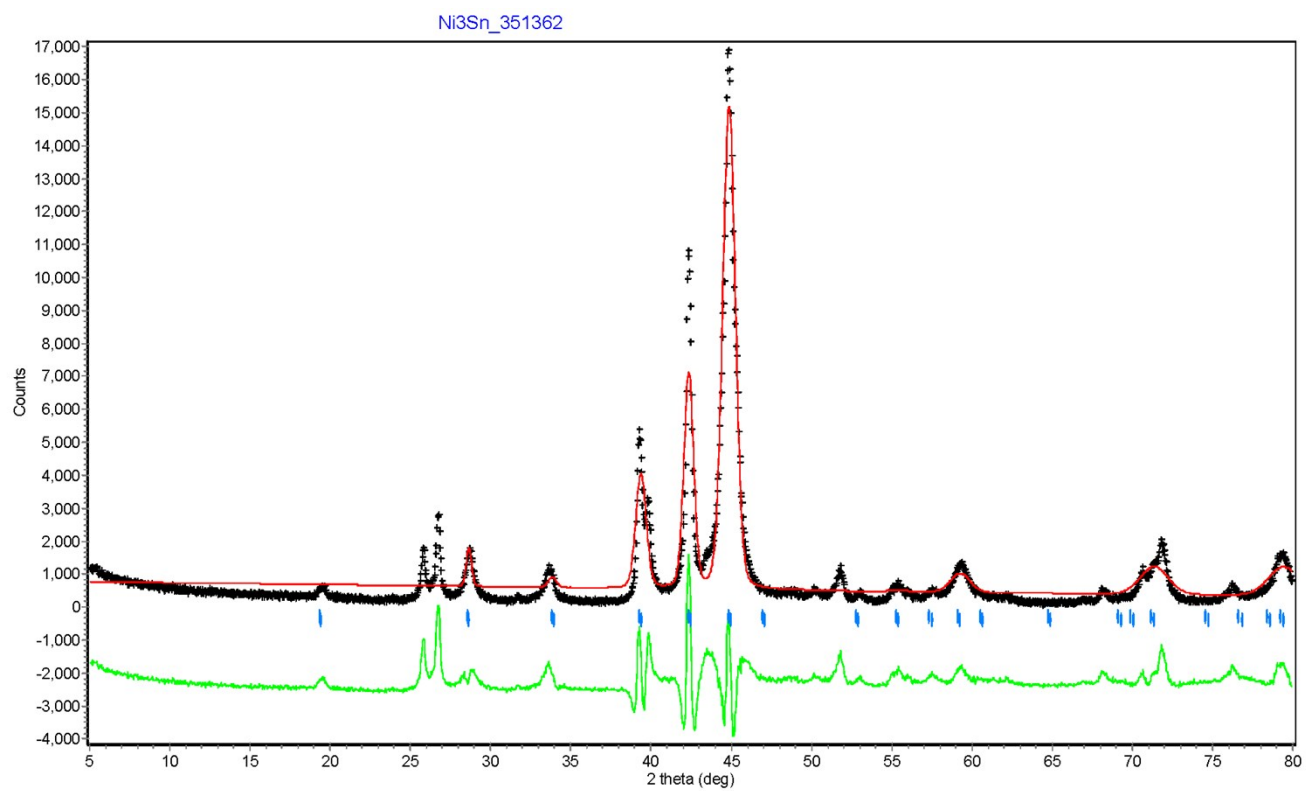


Fig. S3 Le Bail intensity extraction profiles of powder XRD data for Ni-Sn(3.0) alloy catalyst. Data points (+ line); Calculation line (red line); Difference line (green line); Marker points (blue vertical line).^{S6}

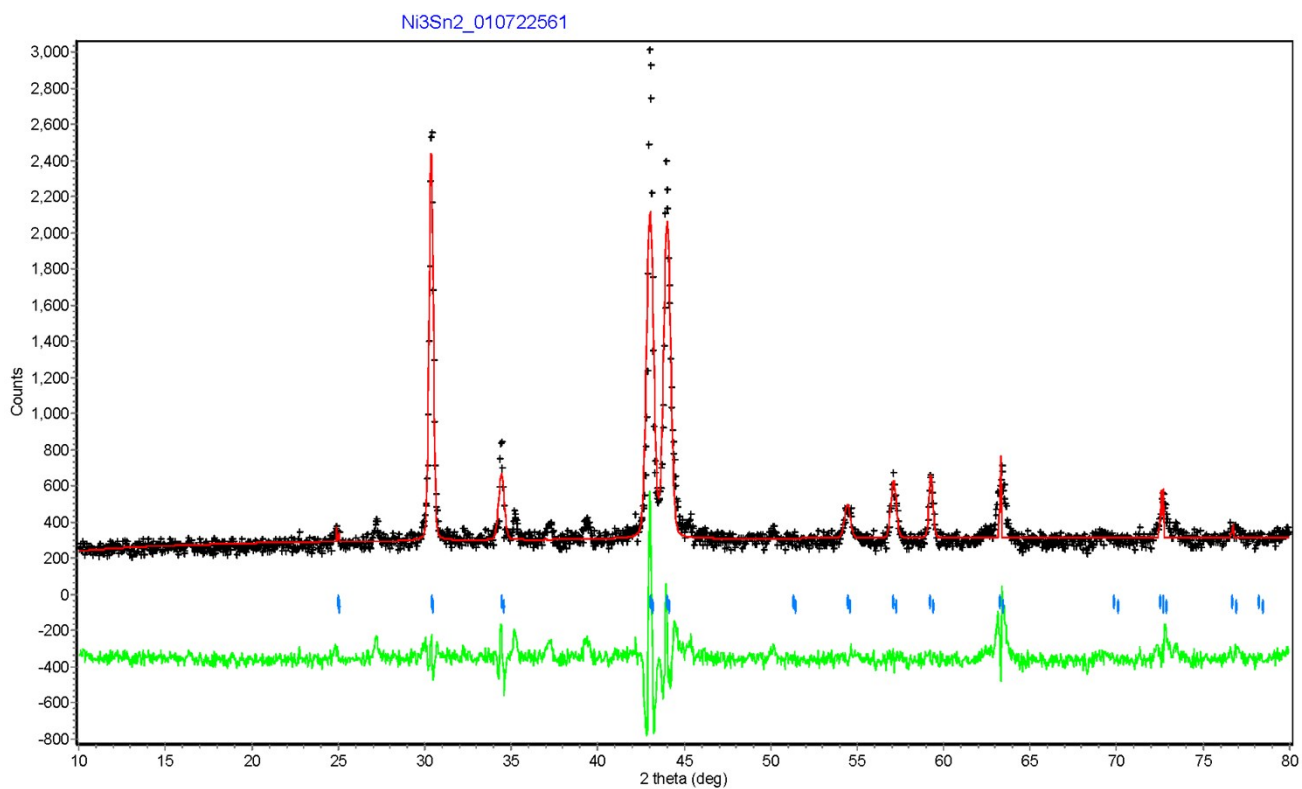


Fig. S4 Le Bail intensity extraction profiles of powder XRD data for Ni-Sn(1.5) alloy catalyst. Data points (+ line); Calculation line (red line); Difference line (green line); Marker points (blue vertical line).^{S6}

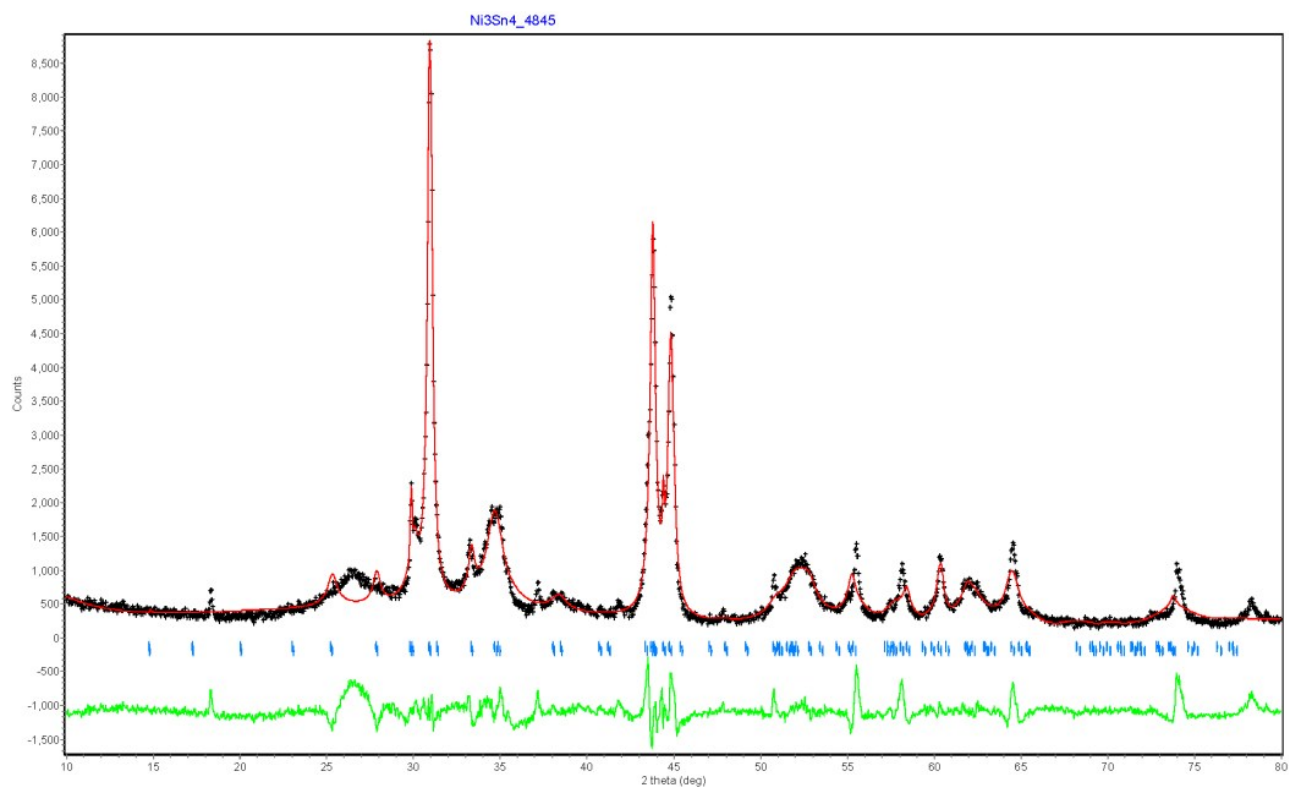


Fig. S5 Le Bail intensity extraction profiles of powder XRD data for Ni-Sn(0.75) alloy catalyst. Data points (+ line); Calculation line (red line); Difference line (green line); Marker points (blue vertical line).^{S6}

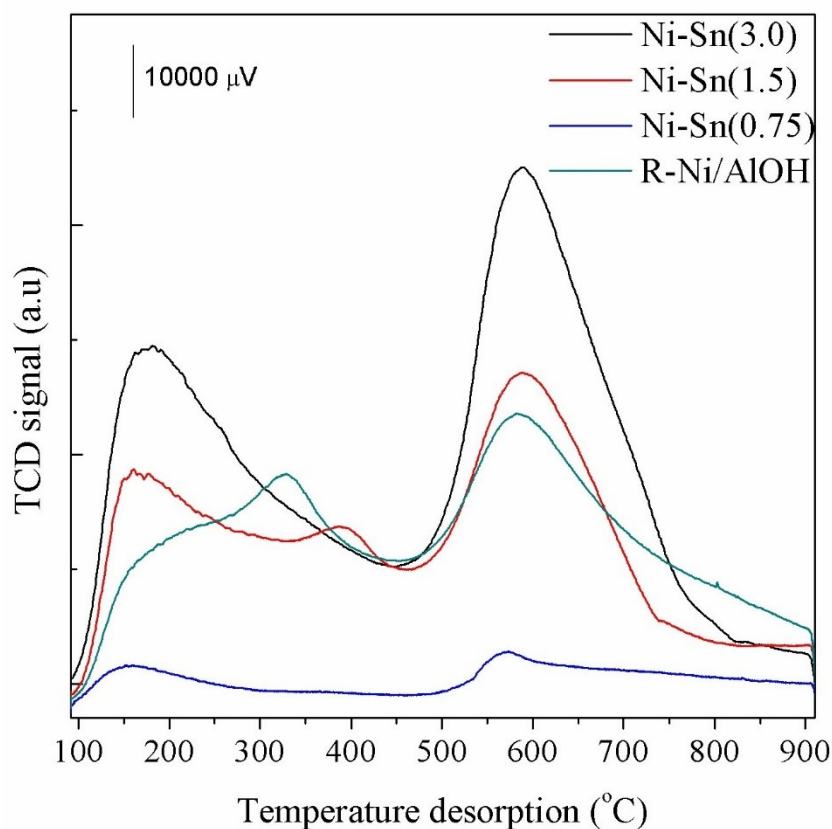


Fig. S6: NH₃-TPD spectra of bulk Ni-Sn alloy catalysts.

Table S2 NH₃-TPD results for bulk Ni-Sn(x) catalysts after H₂ treatment at 673 K for 1.5 h

Entry	Catalyst ^a	Amount of acid sites ^b (μmol/g)
1	Ni-Sn(3.0) (Ni ₃ Sn)	473 (151 weak, 274 medium, and 48 strong acids)
2	Ni-Sn(1.5) (Ni ₃ Sn ₂)	276 (90 weak, 99 medium, and 87 strong acids)
3	Ni-Sn(0.75) (Ni ₃ Sn ₄)	173 (33 weak, 123 medium, and 17 strong acids)
4	R-Ni/AlOH	474 (293 weak, 121 medium, and 60 strong acids)
5	Raney Ni	195 (reference S7)
6	γ-Al ₂ O ₃ (commercial)	180 (reference S8)

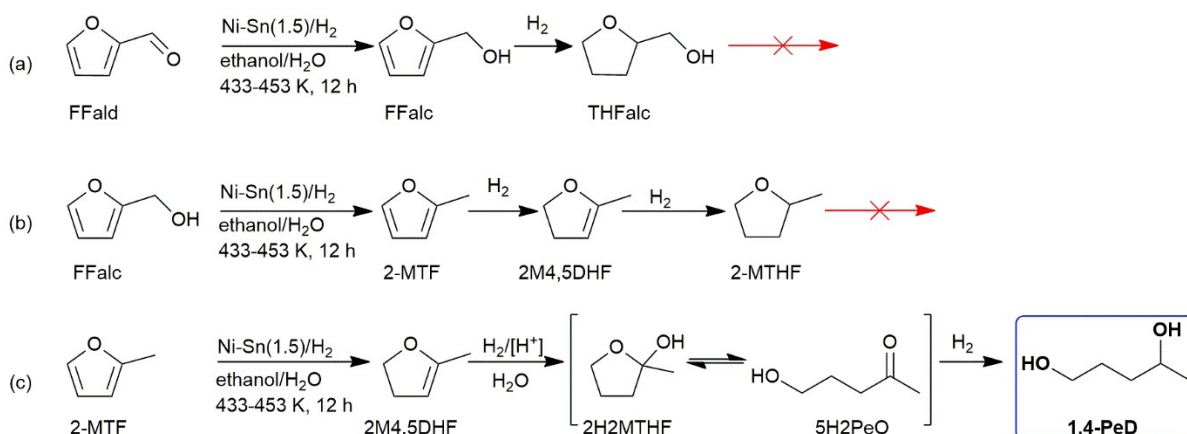
^aValues in the parenthesis are Ni/Sn molar ratio. ^bAmount of acidic sites (μmol g⁻¹) was derived from NH₃-TPD spectra.

3. Results of the catalytic reaction

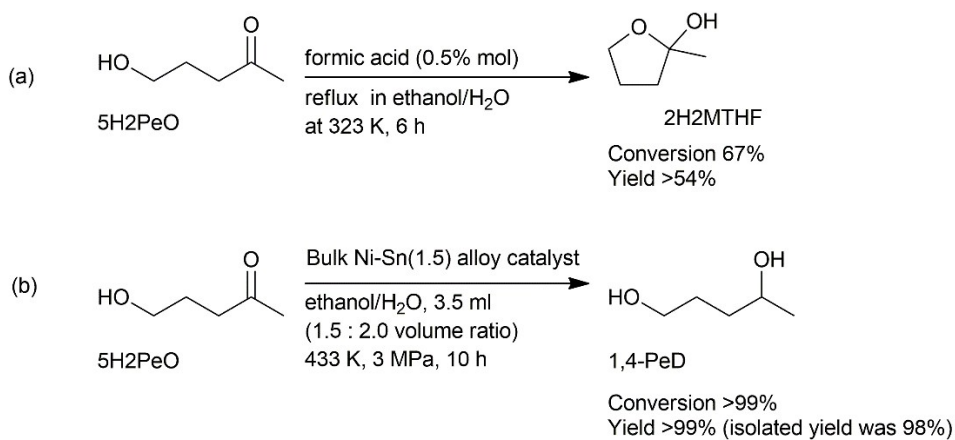
Table S3 Results of hydrogenolysis of various substrates over bulk Ni-Sn(1.5) alloy catalyst.

Entry	Substrate	Conversion ^a / %	Yield ^b /%							
			1,4-PeD	1,2-PeD	1,5-PeD	FFalc	THFalc	HM-MTHF	2-MTHF	Others ^c
1	Furfuryl alcohol (FFalc)	100	67	0	1	-	20	6	0	2
2 ^d	Furfuryl alcohol (FFalc)	100	71	0	2	0	0	26	0	0
3	2-methyl furan (2-MTF)	93	48	-	-	-	-	7	37	1
4 ^e	Tetrahydro furfuryl alcohol	0	0	0	0	0	-	0	0	0
5 ^e	2-Tetrahydro methyl furan	0	0	0	0	0	0	0	-	0
6 ^f	γ -Valerolactone (GVL)	0	0	0	0	0	0	0	0	0
7 ^g	Levulinic acid	100	0	0	0	0	0	0	0	>99

Reaction conditions: catalyst, 44 mg; a substrate, 1.2 mmol; solvent, ethanol/H₂O, 3.5 ml (1.5: 2.0 volume ratio); initial H₂ pressure, 3.0 MPa; 433 K, 12 h. ^aConversion, determined by GC using an internal standard technique. ^bYield, determined by GC and GC-MS. ^cIt may be dimerization product of FFalc according to GC and GC-MS data. ^dTemperature reaction was 453 K. ^eReaction time was 24 h. ^fReaction time was 48 h. ^gThe product was γ -valerolactone (GVL) with a yield of >99%.



Scheme S1 Parallel reaction routes for the synthesis of 1,4-PeD from C5-Furan (FFald, FFalc, and 2-MTF) in the presence of bulk Ni-Sn alloy catalysts in an ethanol/H₂O solvent mixture system.



Scheme S2 (a) Equilibrium reaction of 5H₂PeO and 2H₂MTHF in the presence of formic acid at 323 K, 6 h and (b) Hydrogenation of 5H₂PeO to 1,4-PeD in presence of bulk Ni-Sn(1.5) alloy catalyst at 433 K, 3.0 MPa of H₂, in ethanol/H₂O, 3.5 ml (1.5: 2.0 volume ratio) solvent and a reaction time of 10 h.

Table S4 Comparison of the present work with reported-literatures for the synthesis of 1,4-PeD from C5-furan compounds

Entry	Reactant	Catalyst	Temp/K	P(H ₂)/ MPa	Solvent	Additive	Conv./ %	Yield of 1,4-PeD/%	References
1	Furfuraldehyde	Ni-Sn(1.5)	433	3	Ethanol/H ₂ O	-	100	92	This work
2	Furfuryl alcohol	Ni-Sn(1.5)	453	3	Ethanol/H ₂ O	-	100	71	This work
3	2-MTF	Ni-Sn(1.5)	433	3	Ethanol/H ₂ O	-	100	48	This work
4	Furfuraldehyde	Raney Ni	433	7	Ethanol/H ₂ O	Formic acid	100	25	Ref S9
6	2-MTF	Reduced Ni/Celite	423	8	1,4-dioxane/H ₂ O	Formic acid	100	62	Ref S10
7	Furfuraldehyde	Ru/CMK-3	353	1	H ₂ O	-	100	90	Ref S11

4. ^1H NMR of crude yield of 1,4-pentanediol obtained from FFald after the removal of solvent.

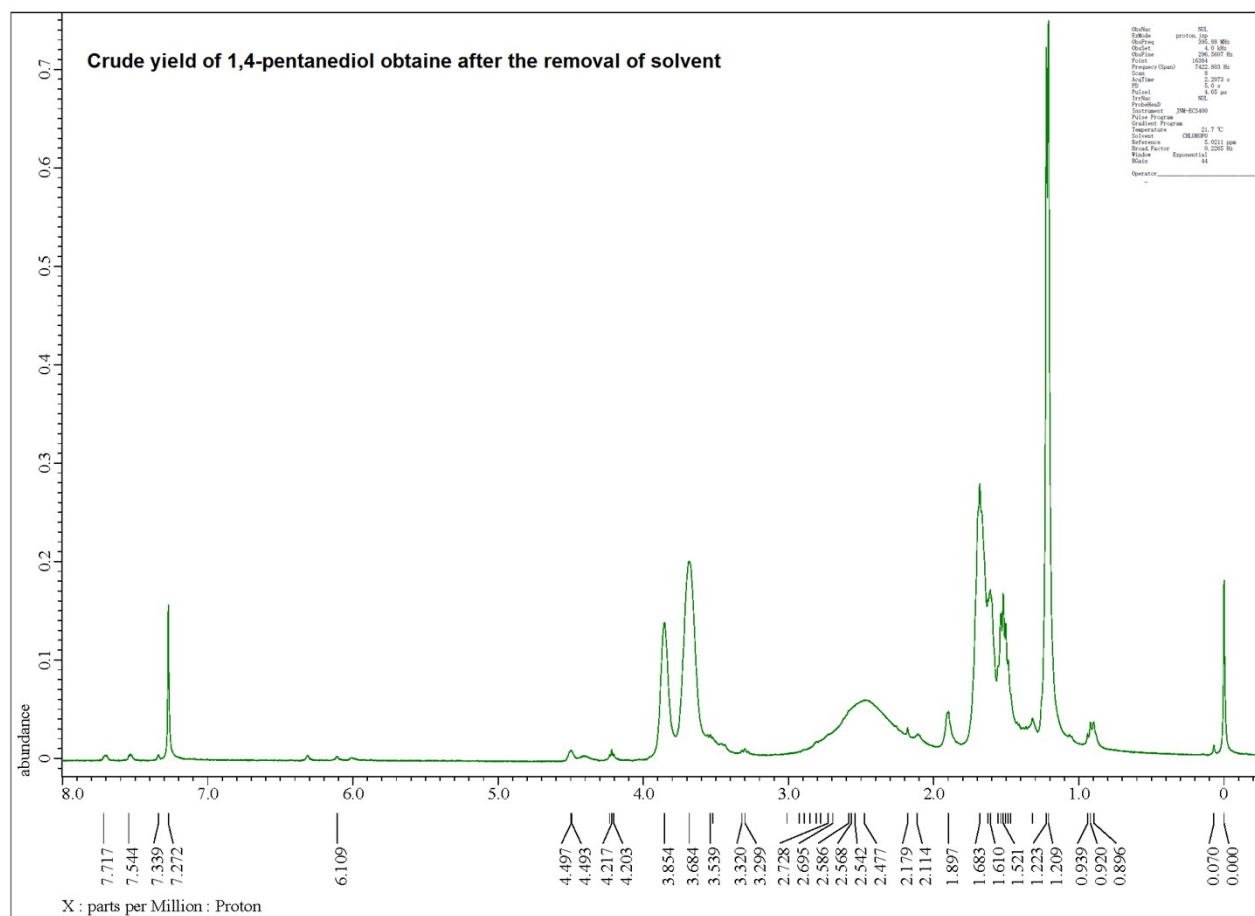
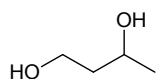


Fig. S7 ^1H NMR of crude 1,4-pentanediol after removal of the solvent from FFald hydrogenolysis over bulk Ni-Sn(1.5) alloy catalyst.

5. ^1H NMR and ^{13}C NMR of isolated product of 1,4-pentanediol obtained from FFald^{S12}



1,4-pentanediol

Yield (92%) GC. Eluent: hexane/ethyl acetate (3:1). ^1H NMR (400 MHz, CDCl_3 , TMS) δ 3.858-3.767 (m, 1H), 3.696-3.585 (m, 2H), 1.677-1.625 (m, 2H), 1.596-1.522 (m, 2H), 1.210-1.175 (d, 3H).

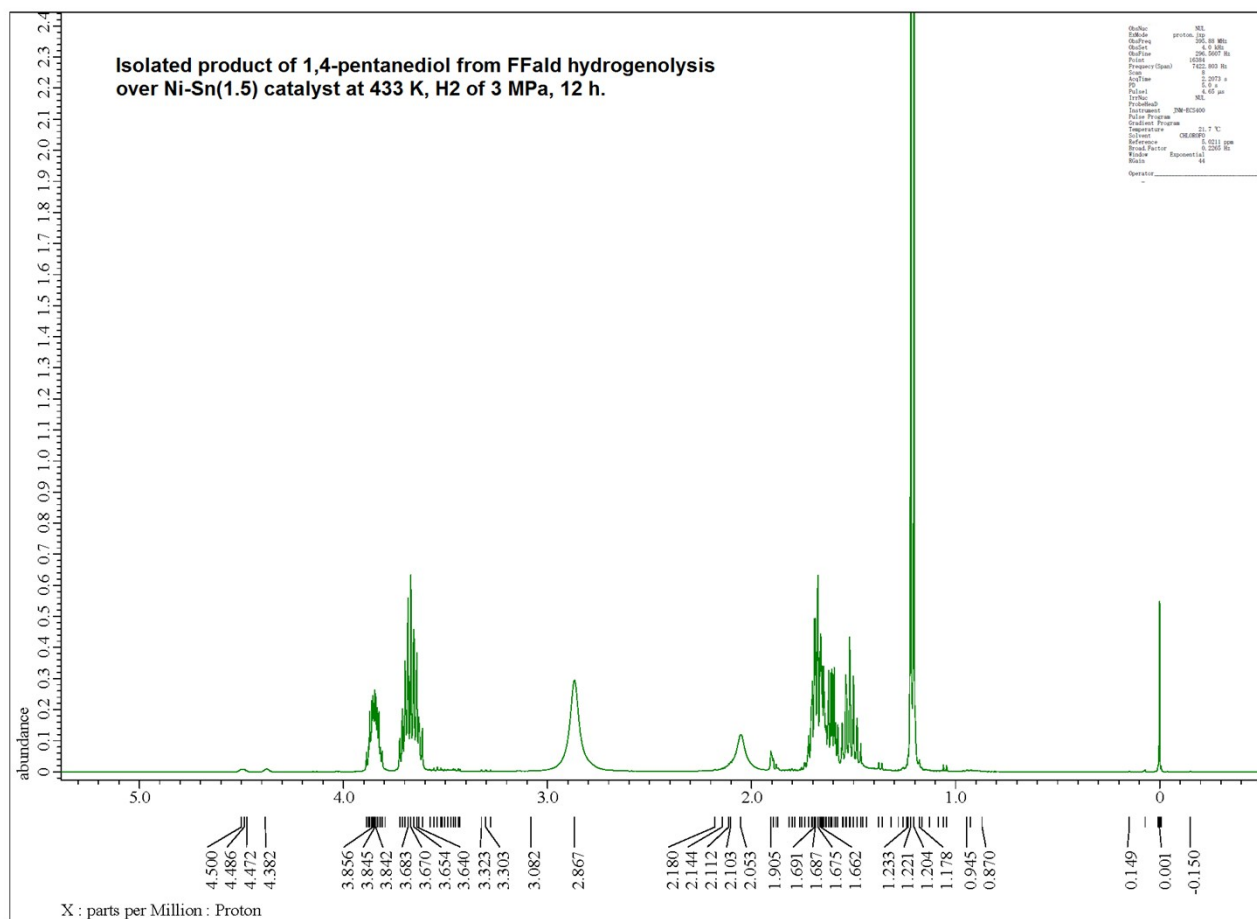
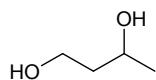


Fig. S8 ^1H NMR of the isolated product of 1,4-pentanediol from FFald hydrogenolysis over bulk Ni-Sn(1.5) alloy catalyst.



1,4-pentanediol

Yield (92%) GC. Eluent: hexane/ethyl acetate (3:1). ^{13}C NMR (CDCl_3 , TMS), δ 67.868 (-CH-OH), 62.713 (CH_2 -OH), 36.281 (- CH_2), 29.134 (- CH_2), 23.520 (- CH_3).

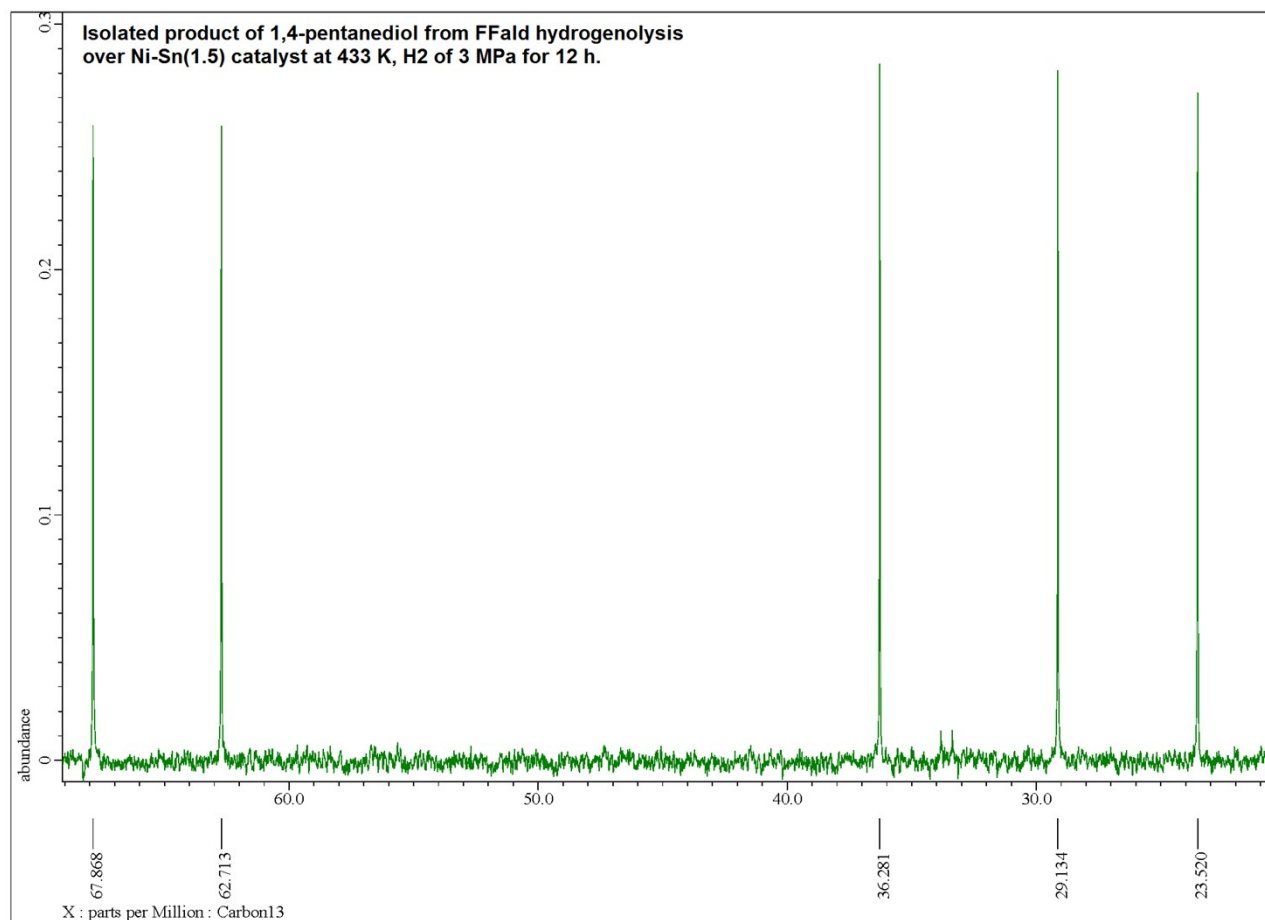
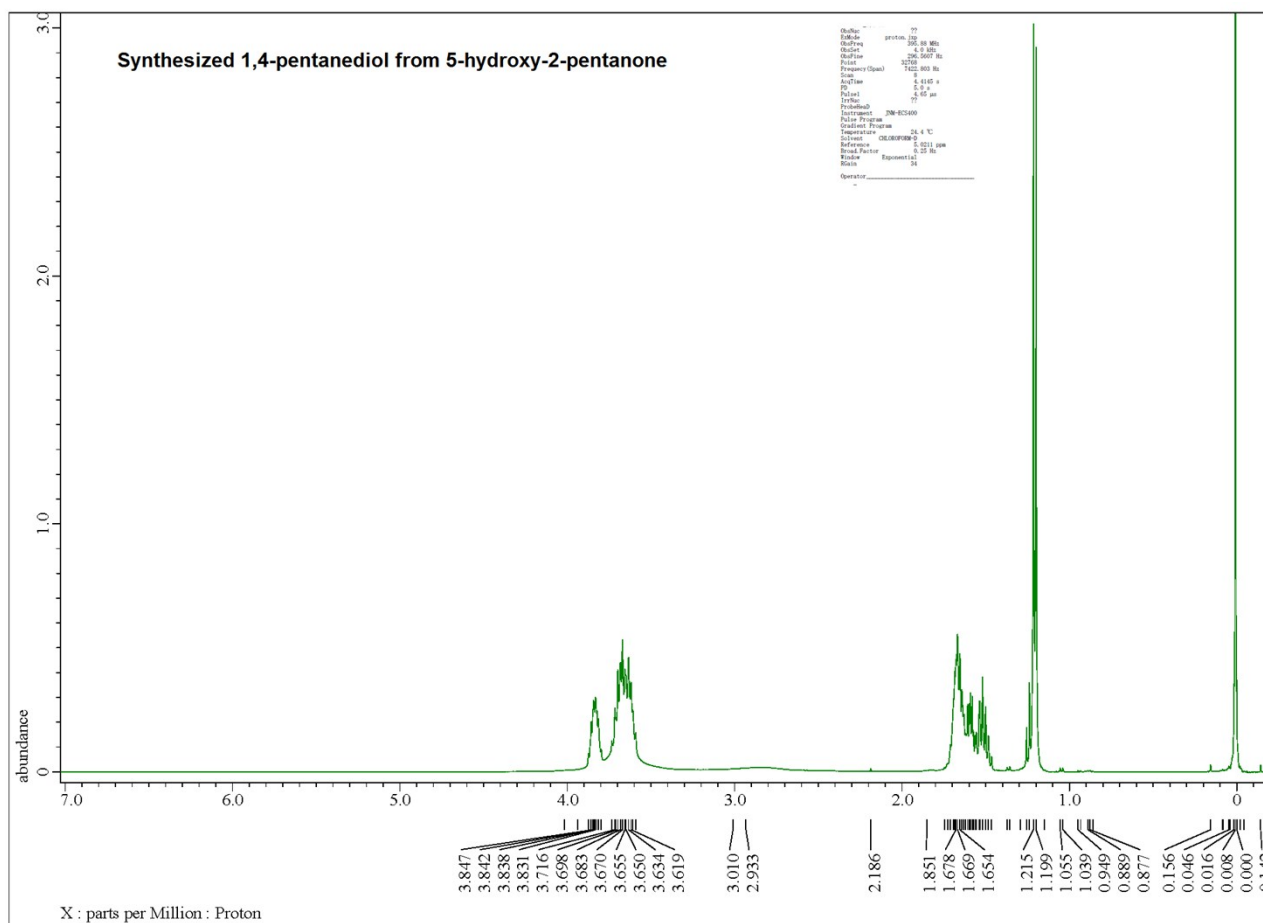


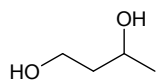
Fig. S9 ^{13}C NMR of the isolated product of 1,4-pentanediol from FFald hydrogenolysis over bulk Ni-Sn(1.5) alloy catalyst.

CC(O)CCO

Yield (98%) GC. Eluent: hexane/ethyl acetate (3:1). (400 MHz, CDCl₃, TMS) δ 3.858-3.767 (m, 1H), 3.696-3.585 (m, 2H), 1.677-1.625 (m, 2H), 1.596-1.522 (m, 2H), 1.210-1.175 (d, 3H).



17



1,4-pentanediol

Yield (98%) GC. Eluent: hexane/ethyl acetate (3:1). ^{13}C NMR (CDCl_3 , TMS), δ 67.858 (-CH-OH), 62.704 (CH_2 -OH), 36.300 (- CH_2), 29.173 (- CH_2), 23.520 (- CH_3).

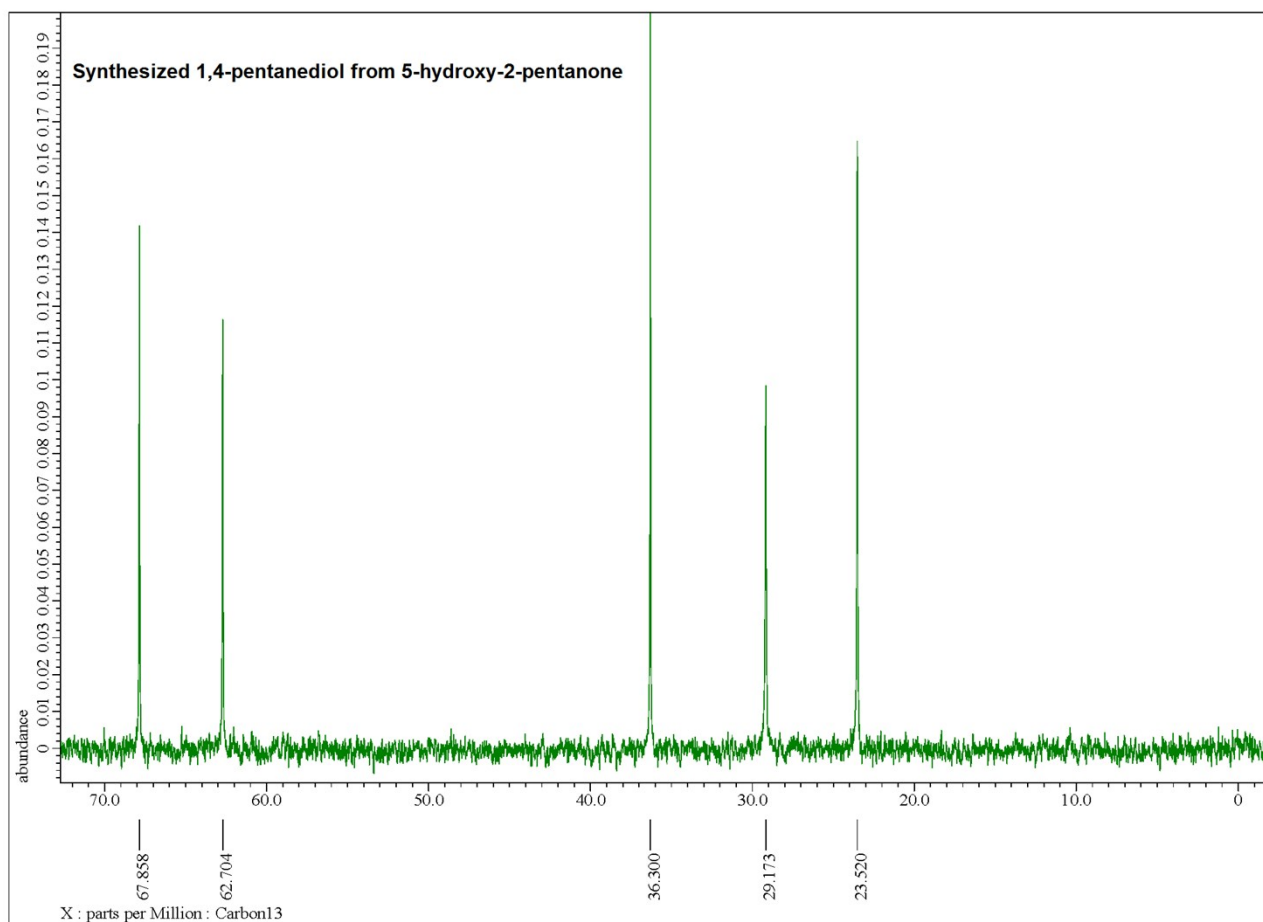


Fig. S11 ^{13}C NMR of the isolated product of 1,4-pentanediol obtained from the hydrogenation of 5-hydroxy-2-pentanone over bulk Ni-Sn(1.5) alloy catalyst.

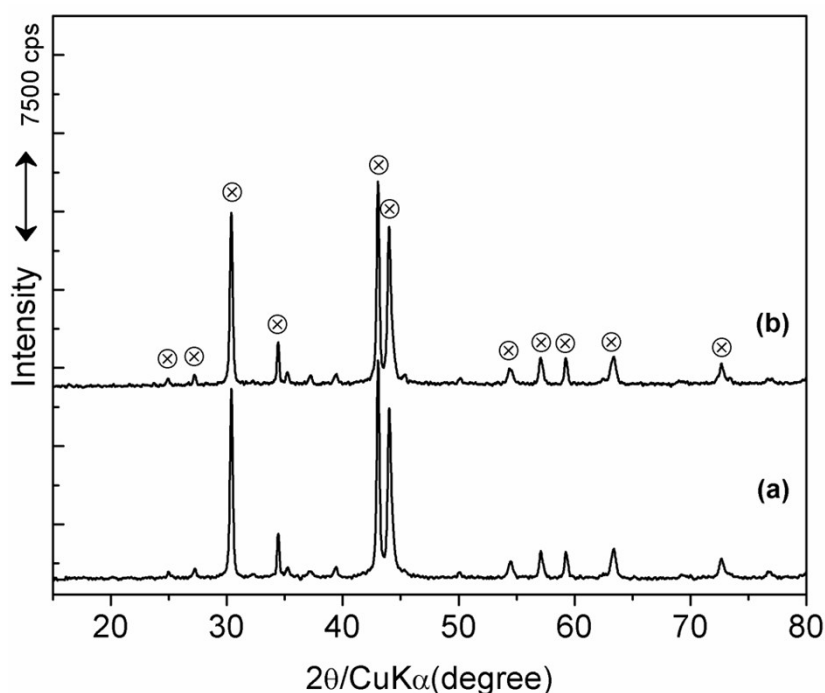


Fig. S12 XRD patterns for recovered bulk Ni-Sn(1.5) before (a) and after (b) H_2 treatment at 673 K for 1 h. (\oplus) Ni_3Sn_2 .

References

- S1. (a) R. Rodiansono, T. Hara, N. Ichikuni, S. Shimazu, *Catal. Sci. Technol.* 2012, **2**, 2139. (b) R. Rodiansono, A. Ghofur, M. D. Astuti, K. C. Sembiring, *Sains and Terapan Kimia*, 2015, **10**(1), 22. DOI: <http://dx.doi.org/10.20527/jstk.v9i1>.
- S2. J. Petro, A. Bota, K. Laszlo, H. Beyer, E. Kalman, I. Dódon, *Appl. Catal. A* **2000**, *190*, 73.
- S3. Powder diffraction file, JCPDS-International center for diffraction data (ICDD), 1991. JCPDS-ICDD 6-414 (Ni_3Sn_2); JCPDS-ICDD 35-1362 (Ni_3Sn); JCPDS-ICDD 4-845 (Ni_3Sn_4).
- S4. T. Hara, M. Hatakeyama, A. Kim, N. Ichikuni, and S. Shimazu, *Green Chem.*, 2012, **14**, 771.
- S5. (a) C.H. Bartholomew, R. B. Pannel, J. L. Butler, *J. Catal.*, 1980, **65**, 335. (b) C.H. Bartholomew, R. B. Pannel, *J. Catal.*, 1980, **65**, 390.
- S6. Rietica Web: <http://www.rietica.org/links.htm/>, Le Bail intensity extraction for powder X-ray diffraction using Rietica software, 2018.01.10.
- S7. B. C. Miranda, R. J. Chimentao, J. B. O. Santos, F. Gispert-Guirado, J. Llorca, F. Medina, F. L. Bonillo, and J. E. Sueiras, *Appl. Catal. B: Enviro.*, 2014, **147**, 464.
- S8. C. Liu, R. Hou, and T. Wang, *RSC Adv.*, 2015, **5**, 26465.
- S9. G. J. Leuck, J. Porkorny, and F.N. Peters, U.S. Patent 2,097,493. Nov 2, 1937.
- S10. (a) L. E. Schniepp, H. H. Geller, R. W. Von Korff, *J. Am. Chem. Soc.*, 1947, **69**, 672. (b) K. Topchiev, *Compt. Rend. Acad. Sci. U. R. S. S.* 1938, **19**, 497. [*C. A.*, 82, 8411 (1938)].
- S11. F. Liu, Q. Liu, J. Xu, L. Li, Y.-T. Cui, R. Lang, L. Li, Y. Su, S. Miao, H. Sun, B. Qiao, A. Wang, F. Jerome, and T. Zhang, *Green Chem.*, 2018, **20**, 1770.
- S12. SDBS Web: <http://riodb01.ibase.aist.go.jp/sdbs/> (National Institute of Advanced Science and Technology, 2018. 02.06).